6

THE STRENGTH OF A COMPRESSIVELY LOADED PLATE BY PHOTOELASTICITY METHOD

J.O. Oladunni, PhD
Department of Civil Engineering
University of Lagos, Nigeria

ABSTRACT

The strength of a square plate under a diagonally compressive load is experimentally examined using a photoelastic method and some optical laws. Lame-Maxwell equations coupled with Filon's transformation, which in essence is a graphical approach, is utilized to separate and interpret the principal stresses. This, of course, is a very powerful method for verifying analytic solutions and also a method for solutions to other complex problems in stress analysis. Many structural loadings of plate serving as columns or structural systems, such as ship and aeroplane structures; shell structures and blades of static and dynamic mechanical equipment with notches, cracks or irregular edges or shapes must have their structural response or behaviour properly predetermined for engineering design irrespective of the existing design code. This technique is very important in obtaining the stress trajectory and it is comparatively simple and less expensive than the usual sophisticated finite element approach that is also capable of producing a similar strength trajectory.

Keywords: Photoelastic method, stress, analysis, notches, cracks, engineering design, strength trajectory, biaxial stress, polariscope, polarizor and analyzer.

NOTATION

F - Photoelastic constant
h - Thickness of material specimen
p - Tensile stresses along directional line of symmetry
Q - Compressive stresses along the direction of applied compression force
P_o, Q_o are stresses at the vertices of the plate.

INTRODUCTION

Initially, the photoelastic optical laws are used to obtain the stress differences corresponding to the fringe numbers. Three specimens of the plate were used to examine the relationship between the varying magnitude of the loads and fringes. From slopes of the linear graphs obtained from the data collected, the optical constraints are obtained.

For a general state of biaxial stress, three independent pieces of information are necessarily utilized. The isochromatic and isoclinic fringes provide full-field visual information which supply two pieces of information at a point. A third is usually in the form of another independent equation in the principal stresses; (i) Maximum stresses on free surfaces where one of the principal stresses is zero and (ii) in the interior points only the stress difference in the principal axis directions are determined from the two sets of fringes. The additional information needed is obtained from shear difference method (finite difference method based on equilibrium equation).

EXPERIMENTAL WORK

The main equipment used is the common photoelastic optical bench consisting of light source, polarizer, first and second quarter wave plates; the camera; the plane and circular polariscopes.

A 3.5" x 3.5" (8.89cm x 8.89cm) square plate whose thickness and photoelastic constant are on average, 1/4in. (6.4mm) and 60psi/in ($0.0163N/mm^2$) is used for the test. Using white light source and crossed polariscope, the isoclinic lines of the square plate loaded between the polarizer and analyzer were obtained. The plate was then loaded to give four distinct fringes in a dark field created by the circularly polarized light of monochromatic green illumination. The photograph of the freezed fringe pattern was then taken and shown in Figure 2. This operation was repeated using bright field instead of dark field. The isochromatic lines of the circular polariscope for both dark and bright field fringes were plotted on a small piece of paper attached to the photographic plate where the fringes were projected. Similarly the isoclinics of the plane polariscope were also superimposed on the previous plot on the photographic plate as shown in Figure.1

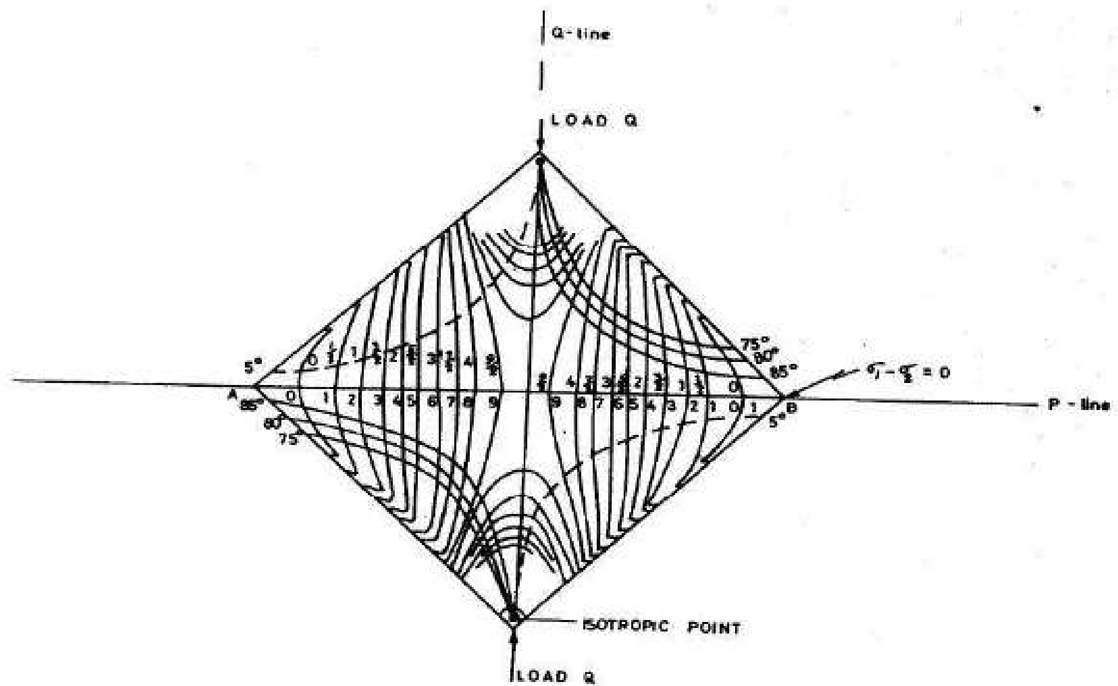

Fig.1: Laboratory Plot of Isoclinics and Isochromatics

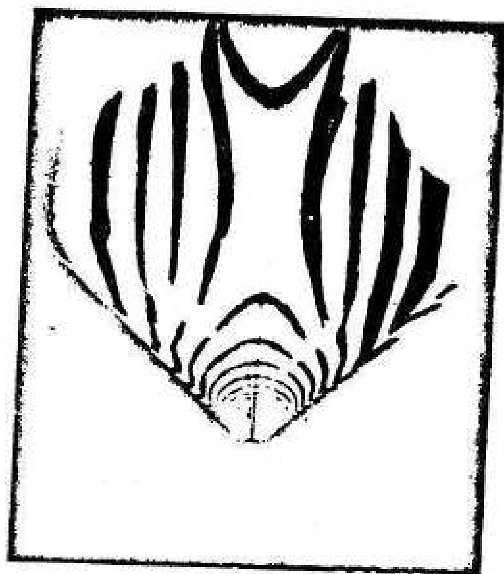

Fig.2: Light Field of Isochromatic Lines

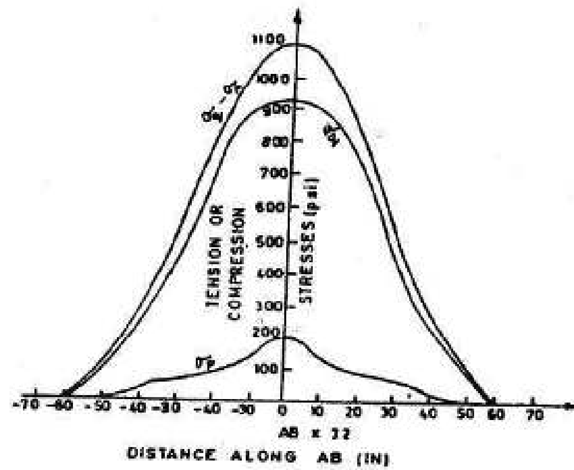

Fig.3: Plots of Principal Stresses and Their Differences Along AB.

Although a 5-degree isoclinic line is necessary for this work, effort was also made to obtain those of 10-degree and 15-degree isoclinics to show the shifts of the isoclinics with the notation of the polarizer and analyzer simultaneously in any direction, but counter-clockwise each time for consistency in operation.

SEPARATION OF PRINCIPAL STRESSES

Theory

The stress at any particular point on the plate along the principal axes is given by Lame-Maxwell equation (1) starting from the intersection of the diagonals. S_o.

Along the P-line

$$(1)\quad P = -P_o + \int_{S_A}^{S_B} \left(\frac{Q-P}{\rho}\right) ds_1$$

$$= -P_o + \sum_i (Q-P) \frac{ds_1}{ds_2} \Delta\phi$$

Along the Q-line

$$(2)\quad Q = -Q_o + \int_{S_A}^{S_B} \left(\frac{Q-P}{\rho}\right) ds_2$$

$$= -Q_o + \sum_i (Q-P) \frac{ds_2}{ds_1} \Delta\phi$$

However, at the vertices of the diagonals, Q_o and P_o are zero. Figure 2 and the computation sheet of Table I show graphical method for obtaining principal stresses along the unloaded diagonal of the plate, using Lame-Maxwell equations along with Filon's graphical techniques.

RESULTS AND CONCLUSION

The results obtained are shown in figure 3, where it is evident that the principal stresses and their differences are markedly maximum and minimum at the intersection of the plate diagonals and zero at the unloaded vertices. Although this is only done for the P-line which is coincident with the unloaded diagonal, it is also obvious that all the P-lines and Q-lines reflect the same bell shape with maximum stresses at the Q-line along the applied load line. One diagonal is compressed while the other is stretched, thus validating the elastic theory.

REFERENCES

1. *Dally, J.W. and Rilley, W.F. "Experimental Stress Analysis", Pub. McGraw-Hill, 1968.*

2. *Timonshenko, S.P. and Goodier, J.N. "Theory of Elasticity", Pub. McGraw-Hill, 1970*

Table 1: Computation Sheet*

No.	N	Q-P	ϕ	$32S_1$	$32S_2$	$(S_1/S_2)\phi$	DEL:P	P	Q
1	2	3	4	5	6	7	8	9	10
1	0	0	.680	10	12	0.57	0	0	0
2	0.5	-120	.253	11	15	0.19	23	12	-108
3	1	-240	.236	7	20	0.08	19	33	-207
4	1.5	-360	.218	5	24	0.05	18	52	-308
5	2	-480	.174	5	27	0.03	14	68	-412
6	2.5	-600	.035	4	30	0.005	3	77	-523
7	3	-720	.052	5	36	0.007	5	81	-639
8	3.5	-840	.157	4	42	0.015	13	90	-750
9	4	-960	.279	5	48	0.029	28	111	-849
10	4.5	-1080	.680	7	60	0.079	65	168	-912

* Note that the variations of stress difference, principal stress along AB are shown in columns 3, 9 and 10 respectively. Figure 3 shows the physical representation of the variations.

Theory: Q-P = NF/h
Q = Compressive stresses along direction of applied compression force.
P = Tensile stresses along directionAB, line of symmetry.
F = Photoelastic constant, 60psi/in per inch (0.0163 N/mm²-mm)
h = Thickness of material specimen, 0.25in. (6.35mm)

7

ORIGIN OF INTERFACE STATES IN SILICON/ SILICON-DIOXIDE SYSTEM - A PIEZOELECTRIC MODEL

Keshaw Singh, MSc. PhD
Associate Professor
Department of Physics,
University of Science and Technology,
Kumasi,Ghana, West Africa

ABSTRACT

The need for higher manufacturing yields and improved operational reliability of Semiconductor Devices and circuits has led to a continuing scrutiny of all processing steps of these Devices. Just like in the bulk of semiconductor, allowed states also occur at the surface of a semiconductor within the energy gap, which are called surface states. A third type of states, similar to surface states, occur at the interface of Si/SiO_2 system. These states are called interface states. Very often they are simply called surface states. The origin of these states is much less understood than that of bulk states.

There is as yet no satisfactory theoretical model for explaining the existence of interface states at Si/SiO_2 interface of MOS Devices. These interface charges have been found to vary, among other things, with the oxide thickness, oxidation temperature and substrate thickness. Since the greatest body of scientific and technological work has been carried out on silicon, Si/SiO_2 interface will be treated predominantly in this present investigation.

A model, based on the piezoelectric response of SiO_2 to thermally-induced external stress assumed to be present during fabrication, has been developed to investigate existence of interface states at Si/SiO_2 interface. To confirm this idea the interface charge density has been computed. The model predicts variations of interface charge density with oxide and substrate thickness which fairly explains the experimental results.

INTRODUCTION

Studies on the surface properties of Metal - Oxide Semiconductor (MOS) structure have been reported by several workers (1-5). As a result of extensive studies using mainly MOS capacitors, MOS transistors and gate controlled diodes, the Si/SiO_2 interface is probably the most well characterized solid - solid interface (6). It is well known that the thermally grown oxide layer on silicon surface is characterized by positive charge in the oxide layer. Deal et. al (7) have indicated that the charge centres are located near Si/SiO_2 interface and the surface states density is not a function of the resistivity of the material. However, the surface charge is found to depend upon the oxide thickness, the oxidation temperature and the annealing treatments. Brotherton et. al. (8) have given experimental results of surface charge and stress in the Si/SiO_2 system. However, in spite of the large volume of work, no satisfactory model has emerged which fully explains the variation of interface charge with oxidation temperature. To reach a better understanding of the basic mechanism involved in the theoretical study of the surface states density, a phenomenological idea is used in which the silicon dioxide has been treated as a piezoelectric material. In the present communication, surface state density has been computed using beam theory and bimetallic strip theory considering SiO_2 a piezoelectric material.

The previous authors (9-11) were of the opinion that piezoelectricity is an inherent property of the crystalline structure, but the work of Murayama (12) indicates that charge injection from the electrodes and their subsequent trapping in the film might be responsible for this effect. Singh et. al(13) in their study on MGOS has shown that SiO_2 can get polarized under electric field at suitable temperature. It has also been shown by Sussner and Drausfeld (14) that PVF_2 film, though glassy in structure, does show piezoelectric character.

TYPES OF INTERFACES

Defects present in the oxide which appear to have a net positive charge is generally named fixed oxide charge. Although at room temperature these centres do not interact with mobile carriers at the silicon surface, they still induce undesirable conducting n-type channels on the surface of the p-type silicon. It has been suggested by Grove et.al. (3) that these centres can increase the radiation sensitivity of the oxide.

The achievable interface-state density has continuously dropped (15) which has been shown in Fig.1.

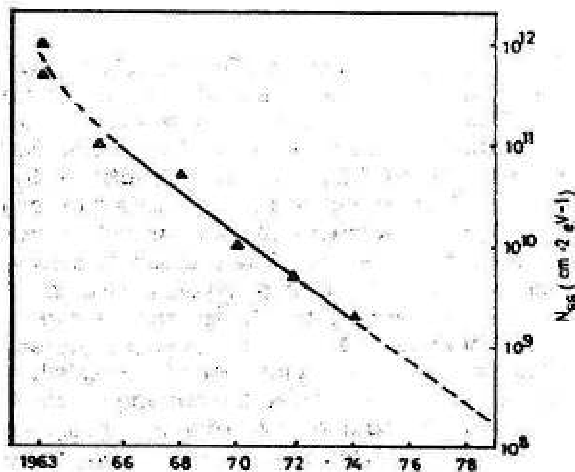

Fig.1: Variation of interface state density with time

The observed improvement in the density has been achieved entirely by empirical methods, without recourse to scientific models of interface states. The improvement is necessary because a low interface-state density is of crucial importance for semiconductor devices. The major spur towards improvement of interface quality has been the MOS technology, which is now in a very advanced state. For most of the MOS devices the present achievable level of interface-state density is more than adequate. However, further improvement is necessary for advanced types of devices, such as charge coupled devices (CCD). There are two different types of interfaces.

1. Interface without states - Intrinsic interface
2. Interface with states - Extrinsic interface

INTRINSIC INTERFACE

For the ideally oxidized SiO_2 - Si interface, it can be imagined that all dangling bonds which cause a high interface state density in the case of a free silicon surface are saturated by bonds with oxygen (16, 17). The strong binding energy of oxygen to silicon shifts the energy of the bonds to lower energies away from the window of the silicon band gap where they are measured electrically (18). It is therefore plausible that the electrically measured SiO_2 - Si interface density is very low, far less than the number of atoms or bonds in the interface. However, it can be easily shown in the schematic arrangement of the bonds in the two dimensional drawing. Fig.2,

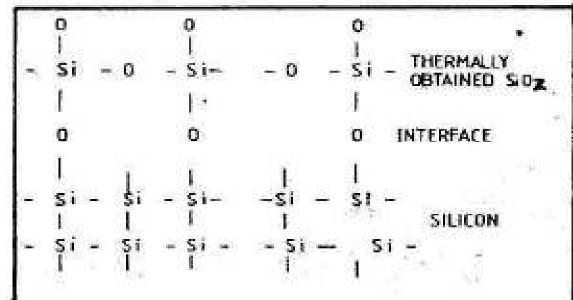

Fig.2: Systematic arrangement of bonds in Si/SiO_2 system

which can be used to represent the 3-dimensional tetrahedral configuration, that the wide lattice of the SiO_2 does not match the lattice of Si. The intrinsic interface states depend mainly on oxidation conditions for thermally oxidized silicon. Dominant parameters which control the interface properties are the technological parameters for the oxide growth. The oxide growth, in the oxidation process of Si, proceeds in three steps (19):

(i) Oxygen transfer into the oxide already formed
(ii) Diffusion of oxygen through the oxide
(iii) Formation of SiO_2 due to reaction of oxygen with silicon at the interface.

Oxidation of Si at higher temperatures (> 1000°C) is diffusion controlled which leads to a square root law for oxide growth. At lower temperature (< 1000°C) the growth is controlled by surface reaction which leads to a linear growth rate. Both types of reactions lead to a thin region of SiO_2 containing partially ionized silicon near the Si/SiO_2 interface where diffusing oxygen reacts to form new SiO_2. There is a thin region with a reduced oxygen concentration (20). The relation of interface states with the oxidation temperature has been explained by Deal (19) and is shown in Fig.3.

A high interface state density is obtained by low-temperature oxidation because there are many unsaturated silicon bonds produced by the slow reaction rate (Fig.3a). A low interface state density is obtained at high temperature because the reaction there is high enough to dominantly produce SiO_2 (Fig.3b). The same low interface state density can be obtained by annealing a low-temperature oxide having excess oxygen (Fig.3c). The annealing, however, must not be too long to avoid depletion of oxygen. Goetzberger et. al. (21) have suggested a 'Charge Model' to interpret interface states. This model explains fast interface states by the binding of mobile charge carriers in the semi-

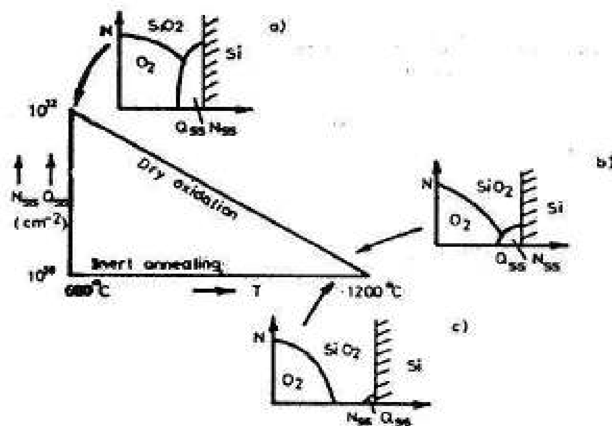

Fig. 3: Relation of interface states with oxidation temperature

conductor to charge centres in the oxide in the immediate vicinity of the interface by Coulomb attraction. A positive charge centre in the oxide will give to a bound donor state analogous to that found in bulk silicon. A negative charge centre will cause an acceptor state.

The random distribution of the depth of the charge centres in the oxide and the partial overlap of their potential will smear out the distribution of the bound states. Centres located deep in the oxide from the state closer to the band edges. Overlapping charges produce deep states. When the energy position is deeper than O.1ev, a distribution of interface states with a high density near the band edges and a drop-off towards midgap is expected.

EXTRINSIC INTERFACE

Impurities may enhance or compensate the oxide charge as well as the number of fast interface states. The property of the impurity depends on its electrical and chemical nature and also its mobility in the interface region. Many elements have a tendency to be gettered in the disturbed region near the interface so that they accumulate in this region even if they are only present in a small concentration.

All the alkali impurities cause a positive space charge in the oxide in the vicinity of the Si/SiO_2 interface. Normally, not all of the impurity atoms are electrically active. An increase of the interface state density proportional to the fixed oxide charge has also been reported. This result supports the "Charge Model" discussed for intrinsic interfaces. However, the increased interface state density could also be caused by additional strain in the Si/SiO_2 interface.

A pronounced effect on interface states is observed for oxidation or annealing in presence of hydrogen (17, 22). These effects can be described by a chemical reaction of unsaturated silicon bonds with water at elevated temperatures under formation of silanol group (22).

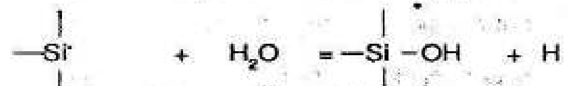

$$-Si^{\cdot} + H_2O = -Si-OH + H$$

A similar reaction is obtained for hydrogen

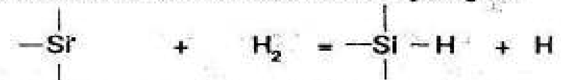

$$-Si^{\cdot} + H_2 = -Si-H + H$$

At temperatures below 500°C annealing in an ambient containing water or hydrogen leads to a reduction of the interface state density. At high temperatures, the reaction is reversed and the interface state density is increased again (22). By varying the partial water pressure, the reaction can be weighted to one side or the other. In presence of hydrogen or water, the annealing triangle is not valid any more because the reaction of hydrogen with oxide charge centres and interface states is different. The oxide charge decreases continuously during annealing even at high temperatures while the hydrogen bond of the above reaction splits again and causes an increase of the interface state density.

The behaviour of other elements is even less well understood. Chlorine itself has no effect on interface state density or oxide charge (23). However, it can be used to bind and neutralize sodium ions which cause an oxide charge (24, 25). Gold is a particularly significant impurity in silicon devices because of its pronounced effects on carrier life time. Gold is also gettered at the Si/SiO_2 interface region during oxide growth (26). It causes some positive space charge and a large interface state density, larger than the number of gold atoms at the interface (26). This behaviour has not been explained properly.

EFFECT OF VARIOUS STRESSES ON INTERFACE STATES

There are some interface states that occur through the preparation technology of the device, which are uncontrolled. Apart from interface states introduced during fabrication process reactive environment, irradiation with x-rays, exposure with light and ion-implantation also increase the distribution of the interface states density. Irradiation increases the thermal vibration of atoms that create electrons and holes in the interface region leading to a build-up of positive space charge in the oxide and increases the interface states density. The electrons drift out of the oxide layer but many holes become trapped. MOS devices with a thin oxide layer (100 A) show little charge trapping; that is,

the number of traps is reduced since holes mays be able to leave the thin-oxide-layer before they are trapped. Ionic implantation of impurities causes great changes at Si/SiO2 interface.

THEORETICAL CONSIDERATION

A linear elastic beam theory for an isotropic material (27) has been used to study Si/SiO2 system. In applying the linear elastic beam theory to Si/SiO_2 system, one can assume the origin of coordination at the Si/SiO_2 interface and adopt the convention that positive and negative stresses represent tension and compression respectively.

Stress on Si:

$$\sigma Si = \frac{P(J)}{D1} + \frac{E1\,D1R(J)}{2}$$

Stress on SiO_2:

$$\sigma ox = \frac{P(J)}{D2} + \frac{E2\,D2R(J)}{2}$$

where E1 - Young's Modulus of Si
E2 - Young's Modulus of SiO_2
D1 - Thickness of Si chip
D2 - Thickness of SiO_2 film

$$P(j) = 2[E1\ I1 + E2\ I2]\ R(j)/H$$

$$H = D1 + D2$$

$$R(j) = \frac{6(\alpha_1 - \alpha_2)(T - T_o)(1 - m)_2}{H[3(1 + m)^2 + (1 + mm)(m^2 + \frac{1}{mn})]}$$

α_1 - coefficient of thermal expansion for Si
α_2 - coefficient of thermal expansion for SiO_2

T - Oxidation temperature
T_o - Room temperature
m - D2/D1
n - E2/E1

I1 and I2 are moments of inertia of Si-chip and SiO_2 - film behaving as beams.

$$I1 = M1\ D1^3/12$$

$$I2 = M2\ D2^3/12$$

M1 and M2 are the masses of Si-chip and SiO_2-film respectively.

COMPUTATION OF INTERFACE CHARGE

From piezoelectronic consideration the charge on Si surface is expressed as (28)

$$Q_{ss} = P_z\ \sigma Si$$

where P_z is the piezoelectric stress constant. The charge state density can be given by

$$Q_{ss} = Q_{ss}/q = P_z \sigma Si/q$$

q - electronic charge

The above discussed method has been used to compute the interface state density for Si/SiO_2 interface. The detailed computer program is given in Appendix 'A'.

RESULTS AND DISCUSSION

The stresses at the interface have been computed as a function of oxide and substrate thickness at 1200°C oxidation temperature. The results of these calculations have been plotted in Figs.4 and 5. For performing the calculations, the necessary physical parameters are given in Table 1 and the computed Q_{ss} in different conditions are given in Tables 2 and 3.

The model has been checked by calculating the variation of charge state density at the interface with oxide film thickness. Surface charge has been calculated for different oxide thickness at T = 1200°C and Si-chip thickness of 0.2×10^{-1}cm. Theoretically charge density is found to decrease with oxide thickness which agrees quite well with the experimental results (29). Experimentally the charge decreases with thickness up to 0.4×10^{-4}cm and afterwards it becomes approximately constant. The variation of surface state density with oxide thickness has been plotted in Fig.4.

The model was further checked by calculating the charge state density by changing the thickness of Si-chip. Fig. 5 shows that the charge state density is practically independent of the Si thickness which fairly explains the nature of experimental results (29).

The question of any inconsistency posed by the results can be eradicated by taking into account the dependence of piezoelectric constant P_z with temperature. P_z decreases by 17% as the temperature rises from 15 to 500°C (30). Hence if P_z is taken as a temperature dependent $P_z = P_z(T)$, the model would certainly explain the experimental results (22) with great accuracy.

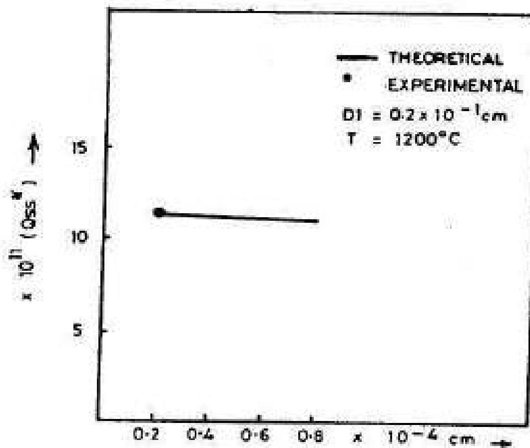

Fig.4: Variation of surface state density with oxide thickness

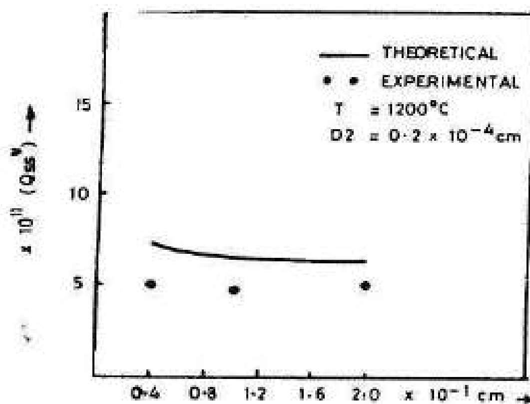

Fig.5: Variation of surface state density with substrate thickness

Table 1:
Physics Parameters

T_o	=	25°C		
E1	=	16.92	x	10^{11} dynes/cm²
E2	=	6.60	x	10^{11} dynes/cm²
α_1	=	2.60	x	10^{-6}/°C
α_2	=	0.50	x	10^{-6}/°C
q	=	1.60	x	10^{-19} Coulomb
P_z	=	2.12	x	10^{-14} Coulomb/cm

Table 2:
Q_{ss} At Different Substrate Thicknesses

D1 (x 10^{-1} cm)	Q_{ss} (10^{11} cm^{-2})
0.4	7.072
0.8	6.527
1.2	6.473
1.6	6.459
2.0	6.455

Table 3
Q_{ss} At Different Oxide Thicknesses

D2 (x 10^{-4} cm)	Q_{ss} (10^{11} cm^{-2})
0.2	11.439
0.4	11.423
0.6	11.407
0.8	11.391

ACKNOWLEDGEMENTS

This work has been supported by: Third World Academy of Sciences (TWAS), Trieste, Italy and UNESCO Regional Office for Science and Technology in Africa (ROSTA), Nairobi, Kenya.

REFERENCES

1. Terman, L.M., Solid State Electronics 5, 285 (1962)
2. Lehovec, K., Slobodskoy, A., and Sprangue, J.L. Phys. Stat. Sol. 3, 447 (1963)
3. Grove, A.S., Deal, B.E., Snow, E.H. and Sah, C.T., Solid State Electronics 8, 145 (1965)
Sah. C.T., Solid State Electronics 8 145 (1965)
4. Zaininger, K.H. and Warfield, G., IEEE Trans.Electron. Devices ED-12. 179 (1965)
5. Badcock, F.R. and Lamb, D.R..Inst. J. Electron 24, 1 (1968).
6. Grove.A.S., Physics and Technology of Semiconductor Devices, J. Wiley & Sons Inc. 1967
7. Deal, B.E., Sklar, M., Grove, A.S. and Snow, E.H. J. Electrochem. Soc.114,266 (1967)
8. Brotherton, S.D., Read, T.G., Lamb. D.R and Willoughby, A.F.W. Solid State Electronics 16. 1367 (1973)
9. Kawai, H., J. Appl Phys. 8. 975 (1969)
10. Ohigashi, H., J. Appl. Phys. 47, 949 (1976)
11. Oshiki, M. and Fukada, E., Jpn. J.Appl. Phys. 15., 43 (1976)
12. Murayama, N., J. Polymer Sci. 13, 929 (1975)
13. Singh, B.R. and Srivastava, R.S., J.Inst. Elect. and Telc Engrs. 19, 471 (1973)
14. Sussner, H. and Draufeld, K., J. Polymer Sci. 16., 529 (1978)
15. CRE Critical Reviews in Solid State Sciences, Jan. (1976)
16. Eastman, D. E. et. al., Phys. Rev. Lett. 28. 1378 (1972)
17. Wagner, L.F., et. al. Phys. Rev. Lett. 28. 1381 (1972)
18. Yudurain, A. and Rubio. J., Phys. Rev. Lett. 26, 138 (1972)
19. Deal, B.E. et. al., J. Electrochem. Soc.121 1980 (1974)
20. Sigmon, T.W., Chu. W.K.C. Luganijo, E. and Mayer, J.W.. Appl. Phys. Lett.24 105 (1974)
21. Goetzberger, A., Heine, V. and Nicollian, E.H., Appl. Phys. Lett. 12, 95 (1968)
22. Mantello, F. and Balk, P., J. Electrochem Soc. 118, 1463 (1971)
23. Schulz, M., Klausmann, E. and Huurle, A., Proc.Conf. Semicon. Interfaces (1975)

24. Kriegler, R.J., 12th Annual Proc. on Reliability Physics Las Vegas (1974)
25. Kriegler, R.J. and Kasagu, D., J. Electrochem. Soc. Japan 41, 466 (1974)
26. Schmidt, P.F. and Adda, L.P. J. Appl. Phys. 45, 1826 (1974)
27. Timoshenko, S., J. Opt. Soc. Am 11,233 (1925)
28. Cady. W.G., Piazoelectricity, Vol.1 & 2, Dover Pub. Inc.. New York (1966)
29. Jaccodine, R.J. and Schlegel, W.A., J. Appl. Phys. 37, 2429 (1966).
30. Freedeniksz, V. and Kazamowsky, J. Piazoelectricity Vol.2 & 3, Dover Pub. Inc. N.Y. (1971)

APPENDIX 'A'

```
10   DIM T1 (8), R1 (8), P (8), S1 (8), S2 (8), S3 (8), S4 (8)
20   PRINT TAB(3); "T"; TAB(11); "1/R"; TAB(23); "P";
30   PRINT TAB(31); "SIGMASI"; TAB(45); "SIGMAX";
40   PRINT TAB(59); "QSS"; TAB (71); "PZZX"
50   REM  T1 REFERS TO STORAGE LOCATION FOR TEMPERATURE
60   REM  R1 REFERS TO STORAGE LOCATION FOR DIFFERENT 1/R
70   REM  P FOR P'S, S1 FOR SIGMASI, S2 FOR SIGMAX
80   REM  S3 FOR QSS AND S4 FOR PZZX
90   D1 = .02
100  D2 = .00002
110  E1 = 1.692E + 12
120  E2 = 6.6E + 11
130  A1 = .0000026
140  A2 = .0000005
150  Q  = 1.6E-19
160  P1 - 2.12E-14
170  TO = 25
180  J = 1
190  M = D2/D1
200  N = E2/E1
210  H-D1 + D2
220  I1=2.328 * D1^3/12
230  I2=2.2 * D2  3/12
240  FOR T = 700 TO 1400 STEP 100
250  T1 (J) - T
260  N1 = 6 * (A1-A2) * (T-TO) * (1-M)^2
270  D=H * (3 * (1 + M)^2 + (1 + M * N) * (M^2 +1/(M * N) ) )
280  R1 (J) = N1/D
290  P(J) = 2/H R1 (J) * (E1 * I1 + E2 * I2)
300  S1 (J) = P(J) /D1 + E1 * D1 * R1 (J) /2
310  S2 (J) = P(J) /D2 + E2 * D2 * R1 (J) /2
320  S3 (J) = P1 * S1 (J) /Q
330  S4 (J) = P1 * S2 (J) /Q
340  PRINT TAB(1); T1 (J); TAB (6); R1 (J); TAB (20); P (J);
350  PRINT TAB (30); S1 (J); TAB (40); S2 (J); TAB (54); S3 (J); TAB (66); S4 (J)
360  .J = J + 1
370  NEXT T
375  PRINT: PRINT: PRINT
380  PRINT TAB (3); "D2"; TAB (13); " 1/R"; TAB (27); "P"; TAB (34); "SIGMASI";
390  PRINT TAB (47); "SIGMAX" ; TAB (59); "QSS"; TAB (71); "PZZX"
400  D1 = .02
410  T  = 1200
420  TO = 25
430  K  =  .00002
440  FOR I = 1 TO 4
450  D2 = I * K
460  GOSUB 1490
470  PRINT, TAB(1); D2;TAB(9); R1(I);TAB(23); P(I); TAB(33); S1(I); TAB (42); S2(1)
480  PRINT TAB (55); S3(I); TAB (67); S4(I)
490  NEXT I
```

```
495   PRINT: PRINT: PRINT
500   PRINT TAB (3); "D1"; TAB(11); "1/R; TAB(25); "P"; TAB(32); "SIGMASI";
510   PRINT TAB (44) ; "SIGMAX"; TAB(59); "QSS"; TAB (71) ; "PZZX"
520   D2 = .00002
530   FOR I - 1  TO 5
540   D1 = .04 * I
550   GOSUB 1490
560   PRINT TAB(1); D1; TAB (7); R1(I); TAB (21); P (I); TAB (31); S1 (I);
570   PRINT TAB (40); S2 (I); TAB (54); S3 (I); TAB (67); S4 (I)
580   NEXT I
590   STOP
1490  H = D1  +  D2
1500  N1 =  6 *  (A1-A2)  *  (T-T0)  *  (1-M) ^ 2
1510  D = H *  (3 * (1 + M)   2 + (1 + M *  N)  *  (M^2 + 1/ (M *  N) ) )
1520  R1 (I) = N1/D
1530  P (I)  = 2/H *  (E1  * I1 + E2  * 12) *  R1  (I)
1540  S1 (I)  =  P (I) /D1  + E1 *  D1 *  R1  /'' /2
1550  S2 (I)  = P (I /D2   + E2 *  D2 *  R[illegible](I) [illegible]
1560  S3 (I)  = P1 * S1  (I)  /Q
1570  S4  (I) = P1  * S2  (I) /Q
1580  RETURN
1590  END
```